Supplementary material

Ambient-Noise Wave-Equation Tomography of the Alps and Ligurian-Provence Basin

A. Nouibat[1], R. Brossier[1], L. Stehly[1], J. Cao[1], A. Paul[1], Cifalps Team, and AlpArray Working Group

[1] Univ. Grenoble Alpes, Univ. Savoie Mont Blanc, CNRS, IRD, UGE, ISTerre, *38000 Grenoble, France.*

Text S1: Comparison with the WET model by Lu et al. (2020)

Supplementary Figure S2 shows that major differences are observed between our V_s model and the V_s model by Lu et al. (2020). A change in shape and amplitude is mainly noticeable in sedimentary basins at 6 km depth, such as the Po basin or the southeast French basin. There are also discrepancies in the covered part of the Ligurian sea in the model by Lu et al. (2020). We observe an overall change in the amplitude of velocity anomalies and their contrast, in the European crust along the Alpine arc, as well as in the Adriatic crust (26 and 36-km depth maps). These discrepancies are primarily due to differences in the initial models and the seismic coverage, and secondly to differences in the inversion schemes, in particular the hierarchical inversion we undertake as compared to the one-band inversion in Lu et al. (2020).

Text S2: Azimuthal distribution of misfit

Figure S5 displays the azimuthal distribution of misfit for the initial (red) and final (blue) models at 8, 20, 35 and 35 s. In Lu et al. (2020), the main difference between the initial and final distributions is an overall correction of the mean value towards zero misfit, in particular at long periods. Our initial distributions are not affected by a shift of the mean value (see also Fig. 11 of the main text). However, we observe an increase of the average misfit with period (as in Lu et al., 2020). The final model improve the fit to the data, with overall smaller average misfits and standard deviations. However, the residual variations, even if small, may be related to anisotropy. Furthermore, the variations presented here are averaged over the whole study region, which may encompass local variations of anisotropy.

Indeed, recent studies on azimuthal anisotropy reveal significant variations in the Alpine region (Kästle et al., 2022; Soergel et al., 2022). Further analysis of anisotropy variations would require computing the distribution of misfits by clusters on specific locations. This could be the topic of a future article.

1 Figures S1 to S5

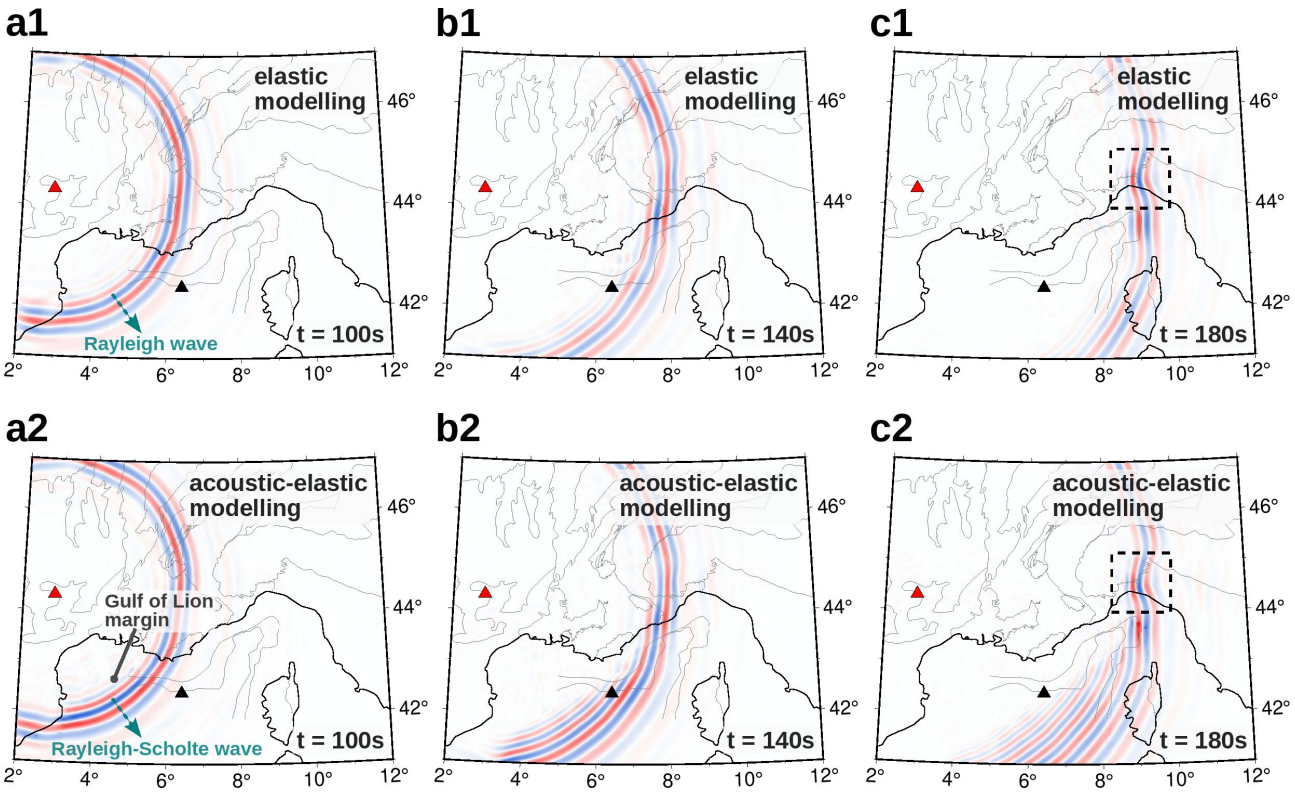

Figure S1: Comparison of snapshots of the vertical displacement wavefield in the 10-20 s period-band simulated using (a1-c1) the elastic wave equation, (a2-c2) the acoustic-elastic coupled wave equation, for the source station indicated by the red triangle. The wave fields are extracted on a 3-D surface corresponding to the topography in the onshore part and to the bathymetry of the sea floor in the marine part. Black dashed frames show scattered Rayleigh-wave packets.

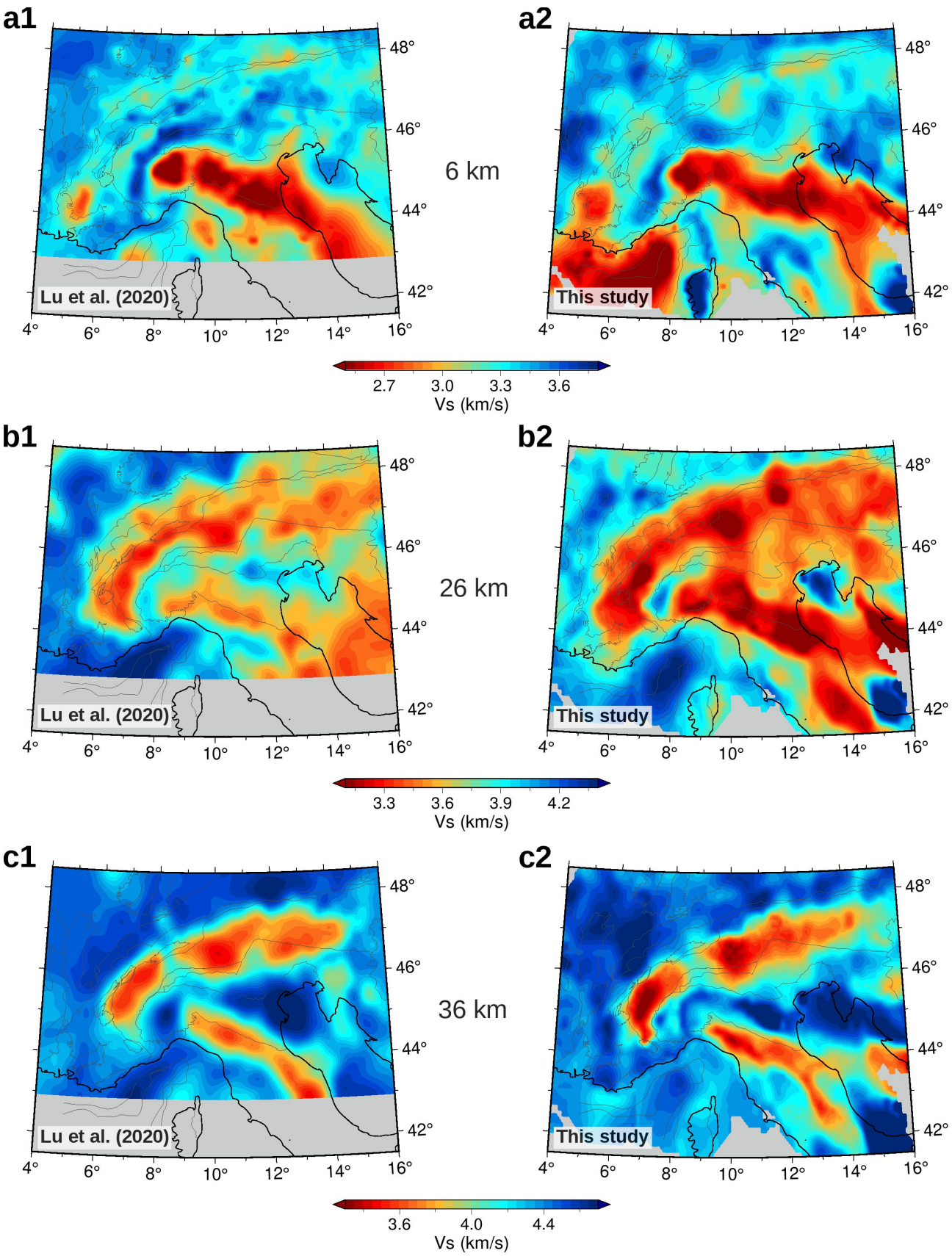

Figure S2: Comparison of depth slices of shear-wave velocities in the WET model by Lu et al. (2020) (a1-c1), the WET model from this study (a2-c2), at 6 (a1-a2), 26 (b1-b2) and 36 km (c1-c2) depths. The gray areas hide regions where the velocity models are unconstrained.

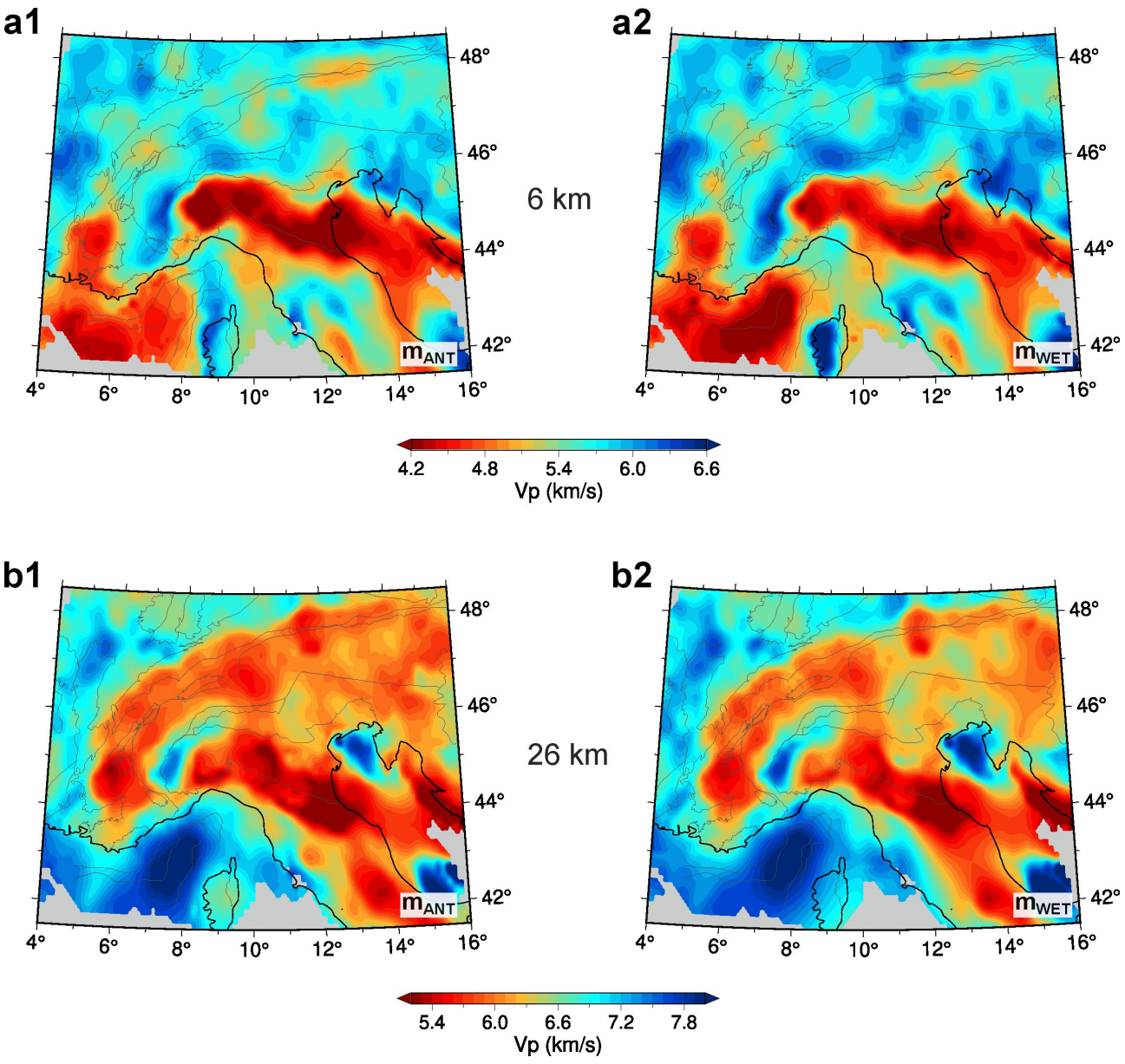

Figure S3: Depth slices in the initial (a1-b1) and final (a2-b2) P-wave velocity models, at 6 km (a1-a2) and 26 km (b1-b2) depths.

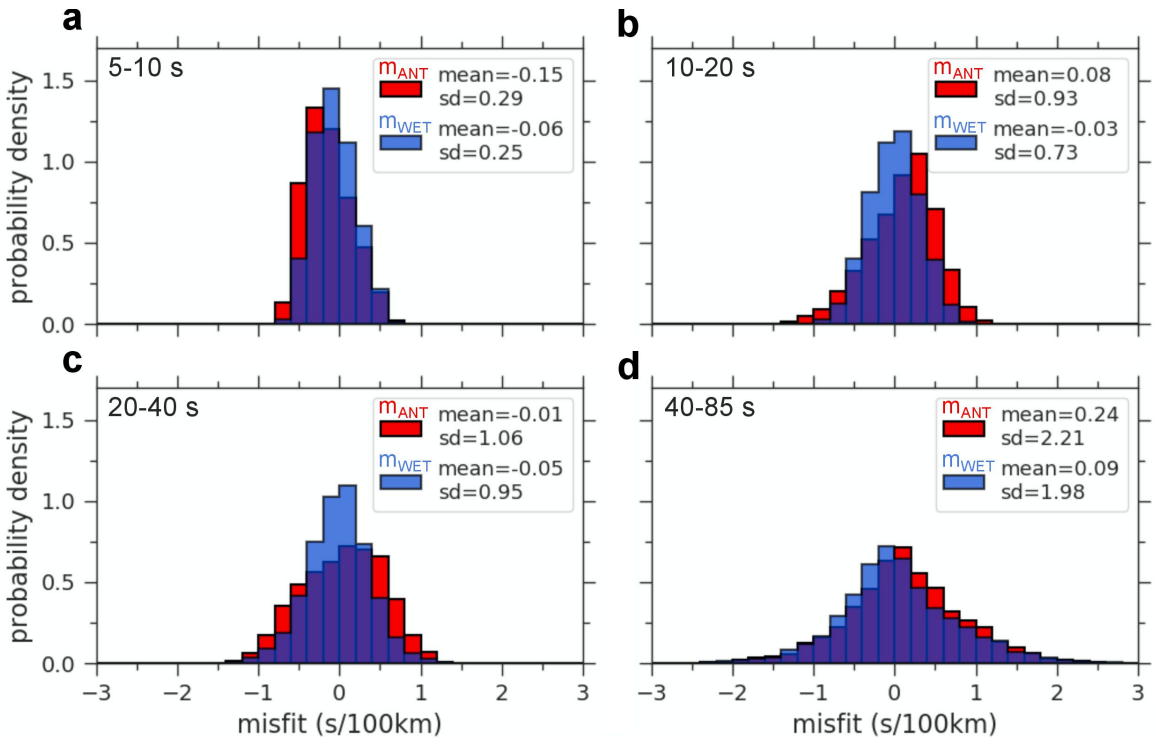

Figure S4: Histograms of cross-correlation type traveltime differences between observed and synthetic waveforms filtered in the period bands 5-10 s, 10-20 s, 20-40 s and 40-85 s. Red: misfits obtained with synthetics computed in the initial model (m_{ANT}), blue: misfits obtained with synthetics computed in the final model (m_{WET}). Labels "mean" and "sd" refer respectively to the mean value and standard deviation of the misfit distribution.

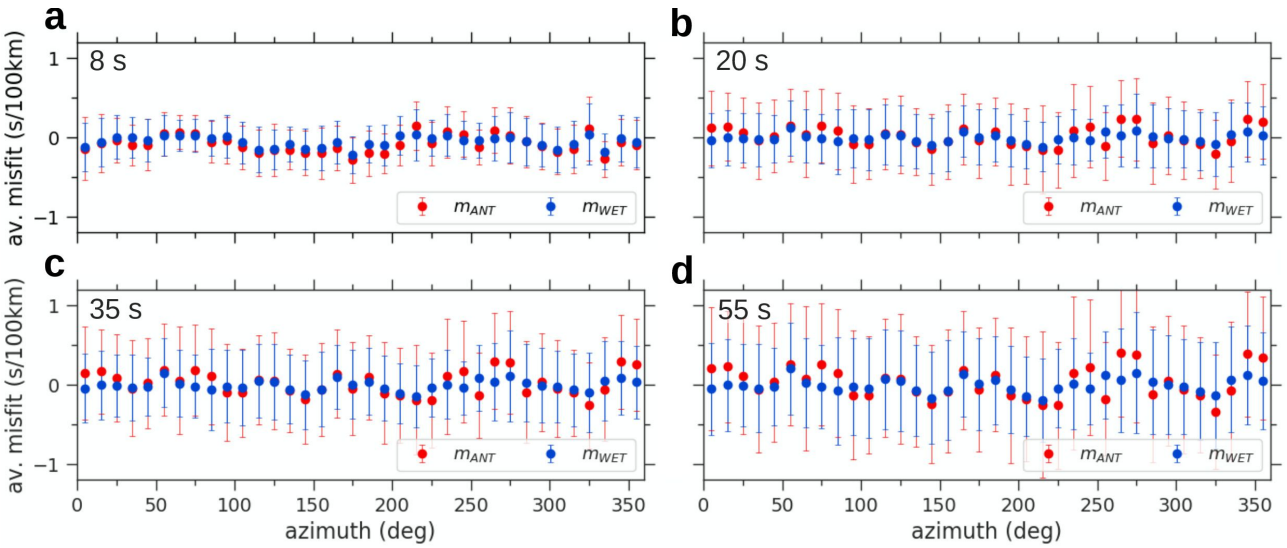

Figure S5: Comparison of the azimuthal distributions of misfit for the initial (red) and final (blue) velocity models at 8, 20, 35 and 55 s periods. Misfits are averaged over uniform azimuth bins of 10 degrees. Error bars represent the standard deviation of the misfits inside bins.

References

Kästle, E., Molinari, I., Boschi, L., Kissling, E., and Group, A. W. (2022). Azimuthal anisotropy from eikonal tomography: example from ambient-noise measurements in the alparray network. *Geophysical Journal International*, 229(1):151–170.

Lu, Y., Stehly, L., Brossier, R., Paul, A., and AlpArray Working Group (2020). Imaging Alpine crust using ambient noise wave-equation tomography. *Geophysical Journal International*, 222(1):69–85.

Soergel, D., Pedersen, H. A., Bodin, T., Paul, A., Stehly, L., et al. (2022). Bayesian analysis of azimuthal anisotropy in the alpine lithosphere from beamforming of ambient noise cross-correlations. *Geophysical Journal International*.